

# Exploring The Structural, Electric And Magnetic Features Of Rare Earth-Doped Copper Ferrite: A Critical Review

M. S. Bisen<sup>a</sup>, A. V. Bagde<sup>b\*</sup>, Y. S. Bopche<sup>c</sup>, D. S. Choudhary<sup>c</sup>, A. M. Shahare<sup>d</sup>, P. B. Wasnik<sup>e</sup>, S. D. Rokade<sup>f</sup>

<sup>a,e,f</sup>*Department of Physics, Yashwantrao Chawhan Arts, Commerce and Science College, Lakhandur, Bhandara, 441803, India*

<sup>\*b</sup>*Chintamani College of Science, Pombhurna, Chandrapur, 442918, India*

<sup>c</sup>*Department of Physics, Dhote Bandhu Science College Gondia, Gondia, 441614, India*

<sup>d</sup>*Department of Physics, S. N. Mor College, Tumsar, Bhandara, 441912, India*

*\*Corresponding author: abagde9@gmail.com*

Copper ferrites doped with rare earth elements exhibit exceptional structural, electric, and magnetic properties, making them a potentially useful material for a wide range of scientific and technological applications. This review provides a comprehensive and critical analysis of the structural, electric, and magnetic features of rare earth-doped copper ferrite. Synthesis methods, structural characterization techniques, and the influence of rare earth dopants on material properties are comprehensively discussed. Specifically, an overview of synthesis techniques and their impact on structural features is provided, alongside a detailed analysis of structural characterization techniques such as X-ray diffraction (XRD), transmission electron microscopy (TEM) and scanning electron microscopy (SEM). The review delves into electrical properties, encompassing conductivity measurements, dielectric analysis, and the effect of rare earth doping on electrical behavior. Similarly, a thorough examination of magnetic properties, such as saturation magnetization, coercivity, magnetic anisotropy, etc., elucidates the impact of rare earth dopants on magnetic features. Additionally, the implications of these properties on the performance of rare earth-doped copper ferrite in applications such as magnetic recording media, microwave devices, sensors, and actuators are explored. Current challenges in understanding and controlling these properties are identified, and future research directions are proposed to address these challenges. The purpose of this review is to provide researchers, engineers, and technologists with a comprehensive resource that provides useful insights into the design and optimization of rare earth-doped copper ferrite materials for advanced applications.

**Keywords:** copper ferrite, X-ray diffraction, saturation magnetization, coercivity, magnetic anisotropy, electrical properties, scanning electron microscopy.

## 1. Introduction

Copper ferrite, which belongs to the spinel group of minerals, is a significant component in materials science due to its unique magnetic and electric properties [1]. This material has been the focus of extensive research owing to its potential applications across numerous technological domains. It has diverse applications in technology, including its use as a

separation tool for various materials, a catalyst for waste gas stream conversion, and a component in power supplies and gas appliances [2]. Its historical development and applications have been extensively studied, with a focus on its physical structure, resistivity, dielectric constant, and magnetic properties [3]. Copper ferrites show promise as anode materials for lithium-ion batteries in the field of energy storage. By combining copper ferrites with reduced graphene oxide, electrodes with a substantial reversible capacity and strong cycling performance are produced, which are essential for improved lithium storage applications. [4]. Copper ferrites, due to their magnetic properties, are suitable for medical applications like hyperthermia treatment of cancer tumors, benefiting from their heat generation abilities in AC magnetic fields [5]. Copper ferrite's electrical and magnetic characteristics have also been explored for use in humidity sensors. The addition of tungsten trioxide to copper ferrite has been reported to enhance its stability and sensitivity, making it a viable material for such sensors [6]. An analysis was conducted on the characteristics and behaviour of copper ferrite nanoparticles, which demonstrated their nanocrystalline structure and indicated their potential for use in magnetic storage media and spintronic devices [7]. Moreover, copper ferrite's exceptional electrical, magnetic, and optical properties have been harnessed for applications in transformers, transducers, inductors, magnetic fluids, sensors and biosensors [8]. Cobalt doping in copper ferrite thin films has been studied to modify its properties for applications in gas sensors, catalysts, and magnetic devices [9]. The substitution of iron with tungsten in copper-zinc spinel ferrite has been examined to improve its electrical properties for use in humidity sensors, demonstrating the versatility of copper ferrite materials in sensor technology [10].

Based on previous studies, rare earth doping has been proven to be essential in altering the structural, electrical, and magnetic properties of ferrite materials making them versatile for numerous applications. The introduction of rare earth elements such as La, Sm, Ce, Gd, and Dy, etc. into ferrite lattices causes various effects due to the size and magnetic moment of the rare earth ions. This study aims to explore the impact of rare earth doping on the structural, electrical, and magnetic features. Rare earth doping induces lattice distortion and phase formation. For instance, when larger rare earth ions substitute into the spinel structure of Mn-Cr ferrite, polarization effects emerge. These effects are discernible through Raman and FTIR spectroscopy [11]. Additionally, the lattice parameters of NiZnCo ferrite exhibit an intriguing trend: they increase up to a certain doping level ( $x = 0.2$ ) and then decrease [12]. Simultaneously, grain size decreases monotonously with increasing doping concentration [13]. The rare earth doping has a substantial effect on the electrical transport properties of ferrite materials. For example,  $\text{Nd}^{3+}$  doping in Mn-Zn ferrite nanoparticles leads to an increase in resistivity. Interestingly, this effect can be reversed upon exposure to  $\gamma$ -radiation [14]. Ahmed et. al. [15] further supported this, showing that rare earth ions can create new sites and increase valence exchange, leading to changes in electrical properties. This finding suggests that rare earth doping provides a means to tailor the electrical behavior of ferrite materials.

The addition of rare earth elements significantly affects the magnetic characteristics of ferrites. The saturation magnetisation ( $M_s$ ) and coercivity ( $H_c$ ) of Ni-Co ferrite materials are highly influenced by the magnetic moment of the rare earth ion. The coercivity increases in proportion to the atomic number of the rare earth ion [13]. In contrast, in NiZnCo ferrite, the

saturation magnetization declines with growing Gd and La doping [12]. Furthermore, cobalt ferrite thin films exhibit magnetic responses directly correlated with the magnetic moment of the rare earth dopant [16]. Jacobo et. al. [17] found that rare earth substitution in NiZn ferrites can lead to local distortion and disorder, affecting the magnetic properties. Lastly, Hashim [18] showed that rare earth ion doping in cobalt ferrites can influence dielectric, magnetic, and impedance properties, with higher doping levels leading to decreased magnetization and increased coercivity. Beyond structural and magnetic changes, rare earth doping influences other material properties. For example, the cobalt ferrite nanoparticles have a high adsorption capacity for dyes such as Congo red, making it useful for environmental purposes [19]. Moreover, optical properties, such as bandgap, are modified by rare earth doping, with specific trends depending on the chosen rare earth element [16]. These insights contribute to material design and hold promise for applications in diverse fields including sensors, actuators, and environmental remediation [11–14,16,19–23].

This review paper aims to thoroughly analyse and evaluate the existing understanding of the structural, electric, and magnetic properties of copper ferrite doped with rare-earth elements. The review aims to assess the influence of rare earth dopants on the structural, electric, and magnetic features of copper ferrite, considering various synthesis methods and doping concentrations. Another objective is to identify the mechanisms underlying the modification of these properties due to rare earth doping, aiming to provide deeper insights into the material's behavior. Furthermore, the review intends to discuss the implications of rare earth-doped copper ferrite in practical applications.

## 2. Synthesis Methods

Common synthesis techniques for these materials include sol-gel, hydrothermal, co-precipitation and solid-state reactions. Each method has its advantages and specific conditions under which it is most effective.



**Fig. 1** Schematic representation of Sol-Gel Autocombustion Method

## 2.1 Sol-Gel Method

Involving the sol-gel procedure, a dispersion colloidal called "sol" is fabricated, and then, subsequently, this dispersion undergoes the gelation, thus ending up in a matrix solidifying into "gel". It offers precise control over the stoichiometry and homogeneity of the final product [24]. This process is incredibly versatile and enables the creation of nanoparticles with exceptional purity. The sol-gel method has been employed by Talebi [25] to synthesize praseodymium-doped copper ferrite nanoparticles, with starch acting as a capping agent, reducing agent, and natural template, which eliminates the need for external surfactants. Thulium-doped copper ferrite nanoparticles were successfully synthesised as well by Hosseini [26] using a similar sol-gel approach, highlighting the method's adaptability to different rare earth dopants. Calvo-De La Rosa et al. [27] has optimized this technique for the synthesis of copper ferrite ( $\text{CuFe}_2\text{O}_4$ ) nanoparticles, where a polymer-assisted approach has been employed to enhance the control over the chemical composition and magnetic properties of the nanoparticles.

An alternative approach for producing rare-earth ( $\text{Pr}^{3+}$ ,  $\text{Sm}^{3+}$ ,  $\text{Eu}^{3+}$ , and  $\text{Gd}^{3+}$ ) doped bismuth ferrite powders efficiently is the solution combustion method. This soft chemistry route is notable for its speed in obtaining oxide powders with enhanced magnetic properties [28]. Low-temperature synthesis methods have been developed by Lisnevskaya et al. [29] to reduce the energy requirements of the process, achieving nanosized particles at significantly reduced temperatures [29]. Hajasharif et al. used this technique to produce nanoparticles with a cubic phase and paramagnetic properties, which are analysed using various characterization techniques [30]. Studies prove the sol-gel method offers the advantage of high purity and control over the material's properties. However, other methods such as solution combustion and low-temperature synthesis also contribute to the field by providing alternative routes for material preparation with distinct advantages in terms of speed and energy efficiency.

## 2.2 Co-precipitation Method

The co-precipitation approach involves the use of aqueous solutions containing metal ions are mixed under controlled pH conditions, leading to the simultaneous precipitation of metal hydroxides. Subsequent calcination results in the formation of ferrite nanoparticles. This method includes the formation of metal cations from a solution, followed by calcination to form the spinel structure [31,32]. This method is particularly lauded for its ability to control the size and distribution of the particles, a critical determinant of the material's magnetic characteristics and it can be executed at room temperature [32].

A range of coprecipitation synthesis techniques have been explored for the production of copper ferrite and related materials. Frolova [33] found that the pH-dynamic mode at pH 11 is optimal for producing magnetic copper ferrite, while Kalia [34] highlighted the importance of pH and temperature in the synthesis of cobalt ferrite. Goldman [35] developed a method for preparing various ferrites, including NiZn, MgMn, and MnZn, with controlled composition and impurity levels. Sriram [36] Focused efforts to produce nanophase copper ferrite through an organic gelation process, studying the effects of pH and cation-carboxylic group ratio on the final product. Modhave et al. [37] have made significant contributions to

this field, demonstrating the synthesis of nanocrystalline rare-earth substituted copper ferrites  $\text{CuRE}_x\text{Fe}_{2-x}\text{O}_4$  (where RE = Nd, Sm, Ho, and  $x = 0.1, 0.2$ ) using the tartarate co-precipitation method. Their research, monitored through thermal studies and FTIR analysis, confirmed the formation of cubic spinel structures, with particle sizes ranging from 26.2 nm to 38.4 nm. Li et al. [38] explored this technique with rare earth elements such as Sc, Gd and Dy and revealed that the grain size ranged from 10.6 to 12.4 nm, corroborating with particle size observations made by Ikram et al. [39]. Explored the impact of doping rare earth metal ions on the structural, electrical, magnetic, and dielectric characteristics of spinel ferrites. Offered comparative analysis on how various rare earth metal ions affect these properties. The study focused on the impact of the ionic radii of dopant  $\text{RE}^{3+}$  ions on the size of the crystallites, grains, and lattice constant.

### 2.3 Hydrothermal Method

The hydrothermal method involves the reaction of metal salts in an aqueous solution under specific conditions of high pressure and temperature. It allows for the formation of well-defined crystalline structures and controlled particle sizes [40].

A range of hydrothermal synthesis techniques have been explored for the synthesis of copper ferrite or copper-based ferrites doped with rare earth elements. Chang-hua (2007) [41] demonstrated the feasibility of recycling and purifying electroplating sludge through the hydrothermal synthesis of compound ferrite. Tsoncheva (2010) [42] and Sang (2021) [43] both investigated the catalytic properties of copper ferrites, with Tsoncheva focusing on the phase composition and transformation of the materials, and Sang exploring the catalytic activity for the thermal decomposition of ammonium perchlorate. Li-ying (2003) [44] Developed a novel technique for synthesising nanoscale ferrite powders, which could potentially be applied to the synthesis of rare earth-doped copper ferrite. These studies collectively highlight the potential of hydrothermal synthesis techniques for the preparation of rare earth-doped copper ferrite or copper-based ferrites, with a focus on recycling, purification, and catalytic applications. Kurian [45] used the hydrothermal method to fabricate Copper ferrite nanoparticles exhibiting a well-controlled size distribution within a specific range of 6–17 nanometres while experimenting with different synthesis parameters, such as pH, heating time, and hydrothermal temperature. It is found that optimal synthesis conditions optimize the magnetic properties. The duration and temperature of hydrothermal reactions have little effects on the structural and magnetic properties of nanoparticles. However, the pH level significantly influences the physical features of the nanoparticles.

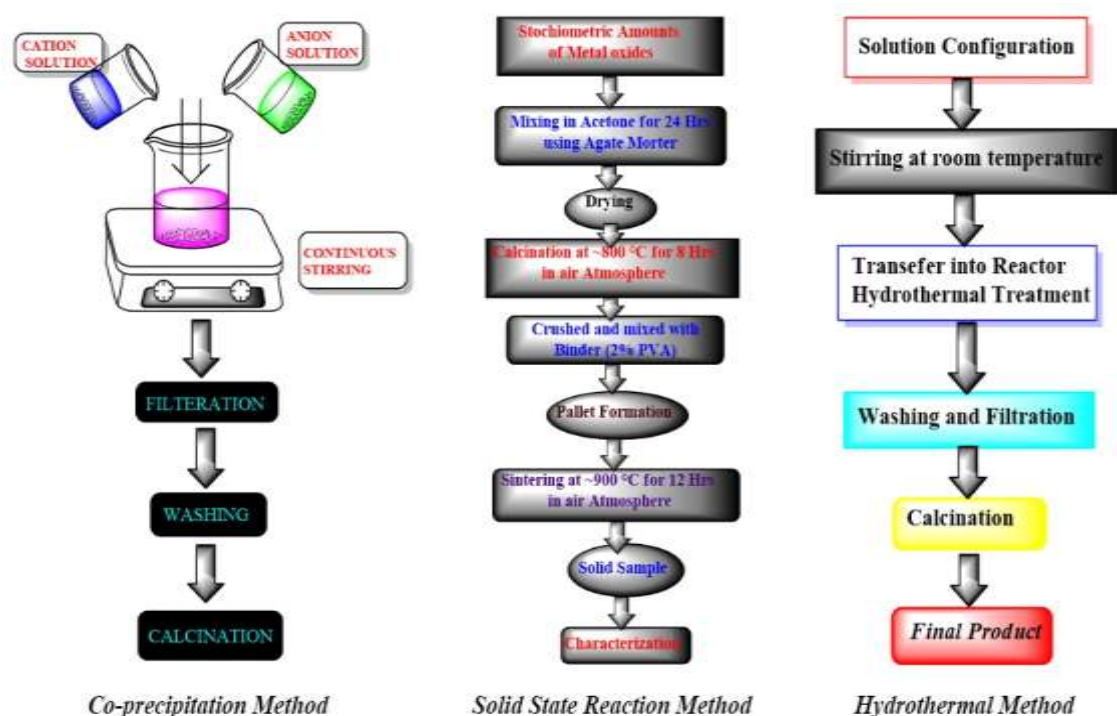


**Fig. 2 Schematic representation of Co-precipitation Method, Solid state reaction Method and Hydrothermal Method.**

## 2.4 Solid-State Reaction

The solid-state reaction method involves the direct mixing and heating of metal oxides or carbonates at high temperatures, leading to the formation of ferrite compounds. This technique is simple and cost-effective but may require high temperatures and a long reaction time [46,47]. The solid-state reaction method is utilized for synthesizing rare earth-doped ferrites, impacting their structural, magnetic, and electrical properties for numerous applications [48]. Solid-state reaction synthesis affects the micro-structure, magnetic properties, and defect evolution of the materials, leading to changes in lattice parameters, bond lengths, and magnetic behavior [49]. Pongpadung (2016) [50] found that the solid-state reaction can result in variations in the microstructural and magnetic properties of copper ferrite. Deraz (2008) [51] further demonstrated that the calcination temperature and the addition of dopants can influence the solid-state reactions in the synthesis process.

## 3. Rare Earth Dopants: Effects on Structural, Electrical, and Magnetic Properties

### 3.1 Lanthanum (La)

The addition of lanthanum to Cu ferrite ( $\text{CuFe}_2\text{O}_4$ ) has been found to significantly impact its structural, electrical, and magnetic properties. The substitution of La into the spinel lattice of



CuFe<sub>2</sub>O<sub>4</sub> can significantly influence the structural, optical, and magnetic properties of the ferrite crystals. Deepapriya et. al. [52] observed that La doping in CuFe<sub>2</sub>O<sub>4</sub> did not inhibit grain growth as efficiently as it did in NiFe<sub>2</sub>O<sub>4</sub>. The UV-visible spectra indicated that the band gap of La-doped CuFe<sub>2</sub>O<sub>4</sub> nanoparticles ranged from 2.1 to 2.3 eV. The magnetic analysis identified variations in the nanocrystals' surface magnetic structures as well as the contribution of the La ion single-ion anisotropy in the crystal lattice. The presence of lanthanum may also influence the bond lengths and bond angles within the crystal lattice, affecting the overall stability and arrangement of atoms.

Furthermore, Dascalu et al. investigated the insertion of rare earth elements, including lanthanum, and found influence on the structural characteristics, coercive field, and saturation magnetization of cobalt ferrite [53]. Studies on other copper-based ferrites, such as Mn<sub>0.5</sub>Cu<sub>0.5</sub>LaFe<sub>2</sub>O<sub>4</sub> and La-substituted Cu<sub>0.5</sub>Co<sub>0.5</sub>Fe<sub>2</sub>O<sub>4</sub>, have shown that lanthanum doping can increase the bandgap energy, dielectric constant, and coercivity while decreasing the field of saturation magnetization [54, 55]. This suggests that similar effects may be observed in lanthanum-doped Cu ferrite. Roy et al. [56] observed that replacing a small portion of iron with lanthanum significantly enhances the magnetic characteristics of Ni–Cu–Zn ferrites, with a significant increase in initial permeability achieved. It also affected density, crystallite size, grain size, and residual macrostress. The solubility of La in the Ni–Cu–Zn ferrite lattice was determined to be extremely low (~0.1 atom/unit cell), producing a secondary phase in the system.

### 3.2 Cerium (Ce)

Hussain et al. exhibited that Cerium doping in Cu ferrite nanoparticles leads to a considerable decrease in crystallite size, cell volume, and lattice constant. This is confirmed by XRD patterns which show a remarkable reduction in these parameters with increasing Ce<sup>3+</sup> content [57]. Similarly, another study using hydrothermal synthesis for Ce<sup>3+</sup> substitution in Cu–Cd ferrites also revealed a reduction in average crystallite size and a slight variation in lattice constant [58]. The substitution also affects the morphology, as observed in SEM and TEM analyses, which show changes in the surface shapes of particles [58]. Some studies revealed the presence of cerium may influence bond lengths and bond angles within the crystal lattice, affecting overall stability and atomic arrangement [57,59]. Optical analysis of cerium-doped copper ferrite samples by Yasmin et al. has revealed the occurrence of two optical energy gaps around 1.6 eV and 2.1 eV. These optical band gaps tend to decrease with Ce<sup>3+</sup> doping, as indicated by redshifts in the optical spectra [59]. Morphological investigation by Khandekar et al. [60] showed the synthesis of very fine spherical nanoparticles of cerium-doped copper ferrite.

The electrical behavior of Ce-doped Cu ferrites changes significantly with doping. The DC electrical resistivities are found to be decreased with an increase in Ce<sup>3+</sup> doping at room temperature [57]. It is evident that the addition of Ce improves the conductivity of Cu ferrites. The dielectric constant and dielectric loss decrease as the cerium concentration increases, suggesting that the ferrites have a semiconducting nature [58]. It is noted that the

ac conductivity has a growing trend with the rise of frequency, suggesting that these materials could be suitable for microwave device applications [57,58].

The magnetic properties of Ce-doped Cu Ferrites are also significantly affected by the  $\text{Ce}^{3+}$  ion substitution. Saturation magnetization ( $M_s$ ) and retentivity ( $M_r$ ) increase with small amounts of  $\text{Ce}^{3+}$  ion doping, showing a notable enhancement in the soft magnetic properties in the study of Hussain et al. [57]. The magnetic property investigation by Rahimi-Nasrabadi, et al. [61] at room temperature also confirms these findings. Yasmin et al. [59] found the weak anti-ferromagnetic nature of cerium-doped copper ferrite. Interestingly, the substitution of cerium reduced the coercivity of copper ferrite, making it suitable for magnetic recording media applications. Cerium-doped Co-Cu-Zn spinel nano ferrites show improved magnetic properties and all magnetic parameters such as initial permeability, coercivity, saturation magnetization, remanence, squareness ratio, Bohr magneton, and anisotropy constant (K) exhibited improved values with increasing Ce concentration [62]. These studies indicate that Ce-doped Cu ferrites have great potential for various applications, such as photocatalysis and microwave technology [57,58,61].

### 3.3 Gadolinium (Gd)

Gadolinium (Gd) doping in ferrites induces significant alterations across structural, electrical, and magnetic properties, as highlighted by various studies. P. Venkata Srinivasa Rao et al. [63] and C B Kolekar et al. [64] observed structural distortions resulting from Gd substitution, impacting crystal symmetry and lattice parameters, consequently influencing magnetic anisotropy and domain structure. In terms of electrical properties, Gd doping affects dielectric response and resistivity. Kolekar et al.[65] reported changes in dielectric constant and resistivity attributed to Gd's impact on charge carriers' mobility and polarization mechanisms. Similarly, Ateia and Soliman [66] noted alterations in electrical conductivity and coercivity due to Gd substitution, affecting conduction and polarization processes.

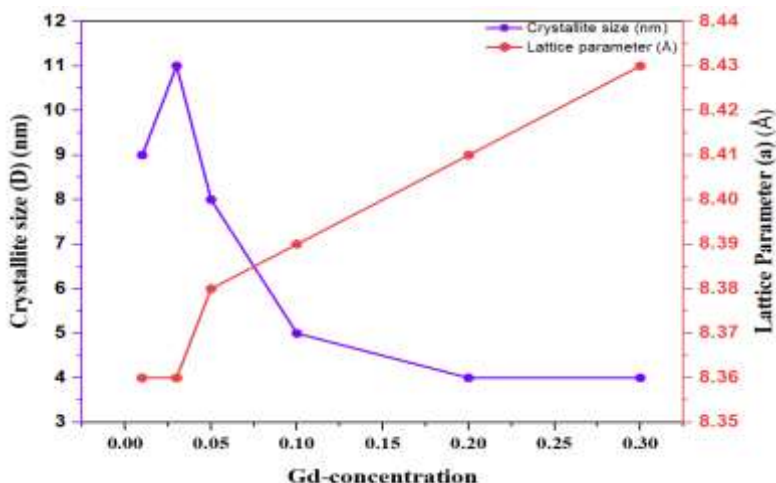




**Fig. 3 Crystallite size and lattice parameter variation with  
Gd-concentration (Bulai et al.) [67]**

Moreover, Gd doping enhances magnetic properties by modifying magnetic interactions and saturation magnetization. Das et al. [68] observed changes in magnetic behavior, including shifts in complex initial permeability, influenced by Gd concentration. This improvement in magnetic properties is crucial for use in magnetic storage devices and high-frequency applications, as emphasized by research conducted by Khanna et al. [69] and Kiran et al. [70]. Additionally, Ruhollah Talebi [71] investigated Gd doping in copper ferrite nanoparticles, noting structural modifications and ferromagnetic behavior induced by Gd incorporation. These findings enhance our understanding of the complex and diverse impacts of Gd substitution on ferrite properties, essential for optimizing ferrite performance for specific technological applications.

### **3.4 Praseodymium (Pr)**

Structurally, Pr doping triggers a transformation from a spinel to an orthorhombic crystal structure because Pr has a greater ionic radius than Fe. This modification of the structure is evidenced by increased grain size in Pr-doped copper ferrite, as observed through XRD and FESEM analysis [72].

Electrically, the addition of Pr dopant affects conductivity and resistivity, albeit detailed electrical characterization may necessitate further specific measurements [72]. Talebi's investigation [73] complements this by highlighting alterations in electrical conductivity and band structure, as evidenced by UV-Vis diffuse reflectance spectroscopy. This suggests modifications in electronic properties that can influence electrical behavior and optical absorption characteristics. Magnetic properties are significantly influenced by Pr doping in copper ferrite. Akhtar et al. [72] demonstrates that as Pr concentration increases, magnetic saturation, coercivity, remanence, and anisotropy constant decrease. Moreover, the coercivity decreases notably with higher Pr content, indicative of superparamagnetic behavior in Pr-doped copper ferrites. Talebi [73] further supports these findings by showcasing ferromagnetic behavior in synthesized nanoparticles, with specific magnetic parameters providing insights into the material's magnetic response.

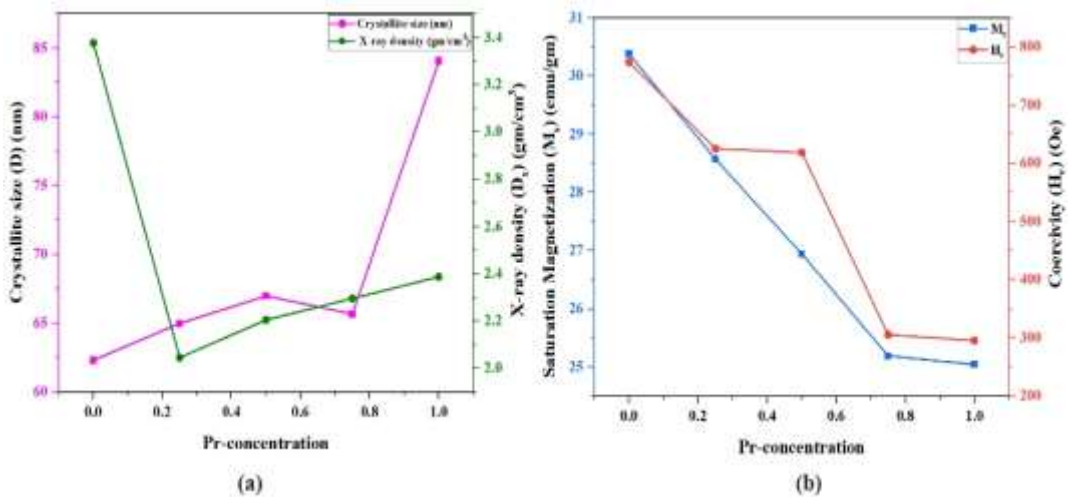


**Fig. 4 (a) Variation of Crystallite size and X-ray density with respect to Pr-concentration (b) Variation of Saturation magnetization and Coercivity with respect to Pr-concentration (Akhtar et al.) [72]**

### 3.5 Neodymium (Nd)

Numerous studies by Ansari et al., Mahalakshmi et al., Vosoughifar and Kimiay, and Rajesh Kanna et al. evidenced that Neodymium (Nd) doping in copper ferrite systems has a profound impact on structural, electrical, and magnetic properties. Structurally, Nd substitution induces notable crystallographic rearrangements, leading to modifications in the lattice arrangement and overall integrity of the materials [74]. Additionally, Nd doping influences electrical transport properties, resulting in significant alterations in conductivity and resistivity characteristics [74,75]. Furthermore, Nd doping exerts a discernible influence on magnetic behavior, leading to modifications in magnetic ordering and interactions within the ferrite structure [74,76,77]. The addition of Nd dopant introduces strains in the crystal lattice, impacting the electrical, magnetic, and dielectric properties of ferrite particles [75]. Mahalakshmi et al. observed changes in electrical conductivity, attributed to enhanced hopping rates between  $\text{Fe}^{2+}$  and  $\text{Fe}^{3+}$  ions, and increased resistivity due to reduced  $\text{Fe}^{3+}$  ions [75]. Moreover, Nd doping influences dielectric behavior, resulting in a significant decrease in dielectric constant across all compositions of Cu-Ni ferrite doped with Nd [75].

Structurally, the introduction of Nd into copper ferrite nanoparticles induces the formation of a tetragonal phase, influencing crystallite diameter and lattice parameters [76]. Electrically, Nd doping affects dielectric parameters, influencing dielectric constant, dielectric loss, and AC conductivity [76]. Additionally, magnetic analysis reveals modifications in magnetic parameters such as remanent magnetization, coercive field, and saturation magnetization, indicative of influence of Nd doping on magnetic behavior [76]. Rajesh Kanna et al. further corroborate these findings, demonstrating alterations in crystal structure, electrical conductivity, dielectric properties, and magnetic behavior induced by Nd doping in copper nano ferrites [77]. The combined findings from these studies underscore the potential

of Nd-doped ferrites as versatile material platforms for the development of advanced functional materials, providing valuable insights for further exploration and application in various technological fields.

### 3.6 Erbium (Er)

In the study steered by Mustaqeem et al. [78], the outcome of Erbium ( $\text{Er}^{3+}$ ) doping on the structural, dielectric, and magnetic properties of copper ferrite ( $\text{CuFe}_2\text{O}_4$ ) nanoparticles was thoroughly investigated. The produced  $\text{CuFe}_{2-x}\text{Er}_x\text{O}_4$  fine powder with varying Er concentrations ( $x = 0.04, 0.08, 0.12, 0.16, 0.20$ ) exhibited notable changes in their properties compared to pure  $\text{CuFe}_2\text{O}_4$ . The lattice parameters and crystallite sizes were found to vary with growing Er doping levels. The  $\text{CuFe}_{1.80}\text{Er}_{0.20}\text{O}_4$  nanoparticles exhibited a crystallite size of less than 50 nm, suggesting that the incorporation of Er caused a decrease in grain size. The increase in dielectric constant with Er doping suggests enhanced dielectric polarization within the nanoparticles. Additionally, the dielectric loss factor and conductivity were found to decrease with Er doping, indicating a reduction in Fe–Fe interactions and changes in the conduction mechanisms within the nanoparticles. The saturation magnetization ( $M_s$ ) of  $\text{CuFe}_2\text{O}_4$  was determined to be approximately 38.01 emu/g. As the  $\text{Er}^{3+}$  content increased, noticeable alterations in saturation magnetization, remnant magnetization, and coercive field were detected. The coercivity and remanence exhibited non-linear behavior with Er doping values, indicating the influence of A–B contacts induced by cationic site modifications.

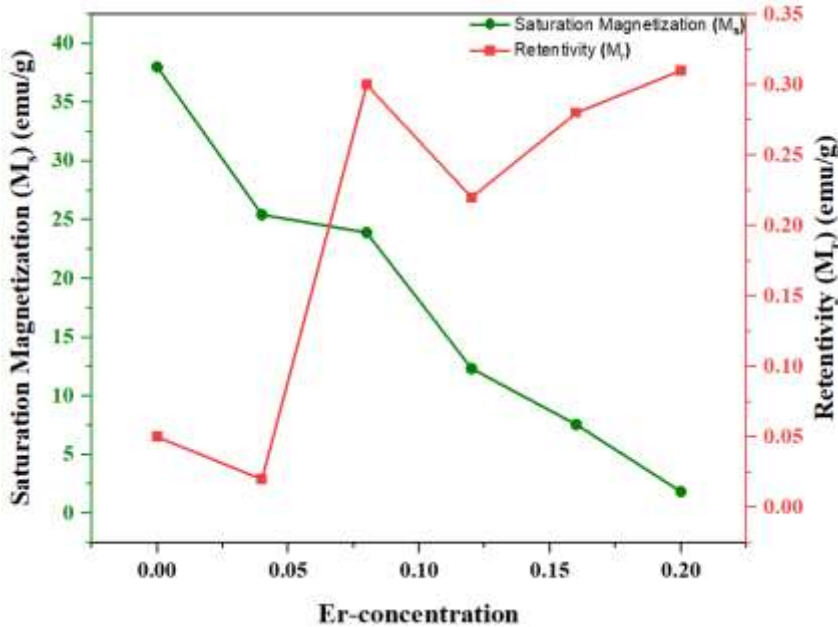


**Fig. 5 Variation of Saturation Magnetization and Retentivity with respect to Er-concentration** (Mustaqeem et al.) [78]

### 3.7 Dysprosium (Dy)

Two studies have thoroughly examined the effects of dysprosium (Dy) doping on the structural, electrical, and magnetic properties of ferrite by Vinod et al. [79] and Hosseini [80]. In the study by Vinod et al. [79],  $\text{Dy}^{3+}$  ion substitution in  $\text{Cu}_{0.8}\text{Cd}_{0.2}\text{Fe}_2\text{O}_4$  nano-ferrites was examined, revealing specific structural, optical, magnetic, and electrical characteristics. The synthesized nanoparticles exhibited a spinel structure, with varying sizes of crystallites 13.82 to 18.32 nm and lattice parameters between 8.349 and 8.385 Å. Optical bandgap measurements showed a semiconducting character, with values in the range of 1.62 eV–1.73 eV. Electron spin resonance (ESR) spectroscopy indicated g-values ranging from 2.613 to 2.333. The magnetic analysis demonstrated a reduction in coercivity ( $H_c$ ) from 557.29–183.89 Oe at 300 K and 749.85–410.72 Oe at 15 K, and the saturation magnetization ( $M_s$ ) has increased from 32.53 to 38.85 emu/g with  $\text{Dy}^{3+}$  concentration. The resistivity values increased from  $9.107 \times 10^6$  to  $1.166 \times 10^8 \Omega\text{-cm}$  with  $\text{Dy}^{3+}$  addition.

In another research investigation done by Hosseini, the effects of Dy doping on the structural, morphological, and magnetic properties of copper ferrite nanoparticles were examined. X-ray diffraction (XRD) analysis established existence of a tetragonal phase, with crystallite diameters around 23 nm. Scanning electron microscopy (SEM) imaging confirmed the morphology and particle size variations induced by Dy doping, with particle sizes ranging from 40–60 nm. Magnetic measurements demonstrated alterations in remanent magnetization ( $M_r$ ) from 9.50 emu/g, coercive field ( $H_c$ ) of 1500 Oe, and saturation magnetization ( $M_s$ ) of 15 emu/g at 300 K. Additionally, electrical measurements indicated changes in resistivity values associated with  $\text{Dy}^{3+}$  doping.

### 3.8 Yttrium (Y)

The effect of Yttrium ( $\text{Y}^{3+}$ ) doping on copper ferrite nanoparticles has been investigated by Moeini et al. [81] through the synthesis of  $\text{CuFe}_{2-x}\text{Y}_x\text{O}_4$  nanoparticles and examined their catalytic properties for click and pechmann reactions. The uniform distribution of Yttrium and Copper ions in the structure enhanced the catalytic efficiency of the nanoparticles without compromising reusability. In the study by Khan et al. [82], Yttrium-doped Copper ferrites were synthesized using the sol-gel method. Morphological and structural analysis confirmed stable tetragonal copper ferrite structures, with the transformation achieved at high sintering temperatures. Raman and FTIR spectra corroborated the tetragonal structure formation with M-O bonding. Electromagnetic response research in the microwave band (1 to 15 GHz) demonstrated a reduction in actual permittivity and permeability with increasing  $\text{Y}^{3+}$  concentration, attributed to variations in crystallinity. The material's low dielectric and magnetic loss tangents make it ideal for low-loss applications. These findings underscore the potential utility of Yttrium-doped ferrite nanoparticles in catalysis and electromagnetic applications.

### 3.9 Europium (Eu) and Scandium (Sc)

The investigations were conducted to evaluate the influence of Eu and Sc co-doping on the structural, electrical, and magnetic properties of copper ferrite. Manjunatha et al. [83] explored the effects of rare lanthanides on the structural, microstructural, and humidity-sensing properties of  $\text{CuEu}_x\text{Sc}_y\text{Fe}_{2-x}\text{O}_4$  ceramics. The samples with varying Eu and Sc

concentrations ( $x = y = 0.00, 0.01, 0.02$ , and  $0.03$ ) were produced using the solution combustion method. XRD analysis revealed a main cubic spinel crystal structure possessing the space group  $Fd3m$ , accompanied by a secondary  $Fe_2O_3$  phase. The spinel crystallite size varied between 25 and 10 nm for different doping levels. SEM studies revealed the porous structure of the prepared samples, with particles that had formed clusters. Hysteresis curves indicated the enhanced resistance and humidity sensing responses with higher concentrations of Eu–Sc doping. The time intervals for capturing the sensor's reaction and restoration were 39 and 40 seconds, respectively, suggesting promising humidity-sensing capabilities of the material. Yousef et al. [84] explored the structural, microstructural, and magnetic properties of  $CuEu_{0.01}Fe_{1.99}O_4$  and  $CuEu_{0.01}Sc_{0.01}Fe_{1.98}O_4$  nanoparticles produced using the self-propagating high-temperature synthesis method. The XRD patterns revealed the presence of a spinel cubic structure with space group  $Fd-3m$ , and the average size of the crystallites was determined to be between 20 and 40 nm. SEM investigations showed that the particles had a porous and agglomerated structure. Energy-dispersive X-ray spectroscopy (EDS) analysis established elemental composition of the samples. Magnetic hysteresis loop measurements indicated a soft ferromagnetic nature, with saturation magnetization, coercivity, and remanence magnetization decreasing with increasing  $Eu^{3+}$  and  $Sc^{3+}$  concentrations. These findings suggest that Eu and Sc co-doping influences the magnetic behavior of copper ferrite nanoparticles, potentially offering tunability of magnetic properties for various applications.

#### **4. Applications of rare earth doped copper ferrite**

Rare earth-doped copper ferrites ( $CuFe_2O_4$ ) are popular due to their unique characteristics and numerous applications. The doping of copper ferrites with rare earth elements such as samarium (Sm), cerium (Ce), gadolinium (Gd), Erbium (Er), etc. has been shown to enhance their magnetic, electrical, and optical characteristics, which can be leveraged in numerous technological advancements. Several studies underscored the multifaceted applications of rare earth-doped copper ferrites and their potential to contribute to significant technological advancements in data storage, optoelectronics, and environmental sustainability.

##### **4.1 Optoelectronics**

One of the prominent applications of rare earth-doped copper ferrites is in optoelectronics domain. The introduction of samarium ions into copper ferrites has been shown to improve the electrical conductivity and optical properties of these materials, making them suitable for use in optoelectronic devices. The enhanced charge density across the grain boundaries and the reduced optical bandgap with increased samarium concentration contribute to these improved properties, which are crucial for applications such as light-emitting diodes and photodetectors due to facilitation of better charge carrier mobility [39,85,86].

##### **4.2 Microwave Absorption and Catalysis**

Rare earth-doped copper ferrites are also being explored by Bian et al. for their potential in microwave absorption, which is essential for reducing electromagnetic interference in communication systems. Moreover, rare earth-doped copper ferrites serve as efficient

catalysts due to their modified structural and electronic properties, which can enhance the reaction rates in various chemical processes [87].

### **4.3 Photocatalysis for Environmental Remediation**

Another application of rare earth-doped copper ferrite is in the field of photocatalysis. Rahimi-Nasrabadi [61] synthesized cerium-doped copper ferrite nanoparticles and found them to be efficient photocatalysts for the degradation of harmful organic dyes under ultraviolet light. This photocatalytic activity is attributed to the unique structural and morphological characteristics imparted by cerium doping. The ability to break down pollutants like methyl orange makes these materials valuable for environmental remediation and water purification process. Additionally, cerium (Ce)-doped copper ferrites have shown promising results as photocatalysts degrade organic contaminants via UV light, which is essential for environmental remediation and water purification [88] .

### **4.4 Magnetic Storage**

Furthermore, rare earth-doped copper ferrites find applications in magnetic storage and electronic devices due to their modified magnetic properties. Doping with rare earth elements such as gadolinium or erbium can enhance the magnetic storage capabilities of copper ferrites, making them suitable for use in high-density storage media [66]. The improved magnetic properties are attributed to the strong magnetic anisotropy and the interplay between the rare earth ions and the ferrite matrix. A study by Li et al. (2021) [38] reveal an increase in saturation magnetization and superparamagnetic behavior at room temperature, which is highly beneficial for high-density magnetic storage applications.

## **5. Conclusion and Future Insight**

In conclusion, rare earth ions like Eu, Sc, Nd, Dy, Pr, Gd, Sm, Y, etc. considerably affect copper ferrite nanoparticles' structural, electrical, dielectric, and magnetic properties. By thoroughly examining the existing literature, it becomes clear that the incorporation of these dopants results in changes to the crystal structure, morphology, conductivity, and magnetic behavior of copper ferrite materials. These modifications offer exciting opportunities for tailoring the properties of copper ferrites to suit specific applications in various technological fields. For instance, Eu and Sc co-doping has demonstrated promising results in enhancing the humidity sensing capabilities of copper ferrite ceramics, indicating potential applications in sensing devices. Similarly, Nd doping has been found to influence the electrical conductivity, dielectric behavior, and magnetic properties of copper ferrite nanoparticles, offering opportunities for use in electronics and magnetic devices. Furthermore, Dy doping has shown potential in altering structural, optical, and magnetic properties of copper ferrite, suggesting applications in catalysis and magnetic recording media.

Future research in this area could focus on exploring novel doping strategies and understanding the underlying mechanisms governing the observed property enhancements. Additionally, further investigations into the specific effects of rare earth ion doping on the microstructure and defect chemistry of copper ferrite could provide valuable insights into



optimizing material performance. Furthermore, developing advanced characterization techniques will enable more precise measurement properties enabling the synthesis and enhancement of copper ferrite-based materials for a wide range of uses. Ongoing studies in this domain hold the potential to drive innovation and advancements in areas such as sensing, electronics, catalysis, and magnetic recording.

## References

- [1] L. Jaswal, B. Singh, *Journal of Integrated Science and Technology* 2 (2014) 69–71.
- [2] R.G. Parker, *Proceedings of the Electrical/Electronics Insulation Conference* (1995) 501–505.
- [3] L. Thakur, B. Singh, *Integrated Research Advances* 1 (2014) 11–13.
- [4] J. Wang, Q. Deng, M. Li, K. Jiang, J. Zhang, Z. Hu, J. Chu, *Scientific Reports* 2017 7:1 7 (2017) 1–12.
- [5] E. Uyanga, D. Sangaa, H. Hirazawa, N. Tsogbadrakh, N. Jargalan, I.A. Bobrikov, A.M. Balagurov, *J Mol Struct* 1160 (2018) 447–454.
- [6] F. Tudorache, *Superlattices Microstruct* 116 (2018) 131–140.
- [7] S. Singh, N. Goswami, S.C. Katyal, *AIP Conf Proc* 2009 (2018).
- [8] S. Balaraman, B. Iruson, S. Krishnmoorthy, M. Elayaperumal, S. Balaraman, B. Iruson, S. Krishnmoorthy, M. Elayaperumal, *Ferrites - Synthesis and Applications* (2021).
- [9] T. Soe, A. Jityen, T. Kongkaew, K. Subannajui, A. Sinsarp, T. Osotchan, *Mater Today Proc* 23 (2020) 752–756.
- [10] I. Petrila, F. Tudorache, *Mater Lett* 108 (2013) 129–133.
- [11] M.H. Abdellatif, A.A. Azab, M. Salerno, *Mater Res Bull* 97 (2018) 260–264.
- [12] X. Zhou, Y. Zhou, L. Zhou, J. Wei, J. Wu, D. Yao, *Ceram Int* 45 (2019) 6236–6242.
- [13] S. Sharma, M.K. Verma, N.D. Sharma, N. Choudhary, S. Singh, D. Singh, *Ceram Int* 47 (2021) 17510–17519.
- [14] P.P. Naik, R.B. Tangsali, *J Alloys Compd* 723 (2017) 266–275.
- [15] M.A. Ahmed, E. Ateia, S.I. El-Dek, *Mater Lett* 57 (2003) 4256–4266.
- [16] G. Bulai, V. Trandafir, S.A. Irimiciuc, L. Ursu, C. Focsa, S. Gurlui, *Ceram Int* 45 (2019) 20165–20171.
- [17] S.E. Jacobo, S. Duhalde, H.R. Bertorello, *J Magn Magn Mater* 272–276 (2004) 2253–2254.
- [18] M. Hashim, M. Raghasudha, S.S. Meena, J. Shah, S.E. Shirsath, S. Kumar, D. Ravinder, P. Bhatt, Alimuddin, R. Kumar, R.K. Kotnala, *J Magn Magn Mater* 449 (2018) 319–327.
- [19] X. Wu, Z. Ding, N. Song, L. Li, W. Wang, *Ceram Int* 42 (2016) 4246–4255.
- [20] B. Zheng, J. Fan, B. Chen, X. Qin, J. Wang, F. Wang, R. Deng, X. Liu, *Chem Rev* 122 (2022) 5519–5603.

- [21] K. Tanbir, M.P. Ghosh, R.K. Singh, M. Kar, S. Mukherjee, *Journal of Materials Science: Materials in Electronics* 31 (2020) 435–443.
- [22] M.H. Abdellatif, G.M. El-Komy, A.A. Azab, *J Magn Magn Mater* 442 (2017) 445–452.
- [23] X.C. Zhong, X.J. Guo, S.Y. Zou, H.Y. Yu, Z.W. Liu, Y.F. Zhang, K.X. Wang, *AIP Adv* 8 (2018) 47807.
- [24] C. Liu, Q. Tian, L. Liao, *Solution Processed Metal Oxide Thin Films for Electronic Applications* (2020) 41–61.
- [25] R. Talebi, *Journal of Materials Science: Materials in Electronics* 27 (2016) 6974–6978.
- [26] S. Akbar Hosseini, *Journal of Materials Science: Materials in Electronics* 27 (2016) 7433–7437.
- [27] J. Calvo-De La Rosa, M. Segarra, *ACS Omega* 4 (2019) 18289–18298.
- [28] A.I. Iorgu, F. Maxim, C. Matei, L.P. Ferreira, P. Ferreira, M.M. Cruz, D. Berger, *J Alloys Compd* 629 (2015) 62–68.
- [29] I. V. Lisnevskaya, I.A. Bobrova, A. V. Petrova, T.G. Lupeiko, *Russian Journal of Inorganic Chemistry* 57 (2012) 474–477.
- [30] P. Hajasharif\*, K. Ramesh, S. Sivakumar, P. Sivagurunathan, *International Journal of Innovative Technology and Exploring Engineering* 9 (2019) 33–37.
- [31] S. Gaffar, A. Kumar, U. Riaz, *J Electroceram* 51 (2023) 246–257.
- [32] M.A. Albalah, Y.A. Alsabah, D.E. Mustafa, *SN Appl Sci* 2 (2020) 1–9.
- [33] L. Frolova, V. Gevod, *Molecular Crystals and Liquid Crystals* (2023).
- [34] S. Kalia, N. Prasad, S. Kalia, N. Prasad, *JETIR* 6 (2019) 1198–1200.
- [35] A. Goldman, A.M. Laing, *Le Journal de Physique Colloques* 38 (1977) C1-297.
- [36] D. Sriram, R.L. Snyder, V.R.W. Amarakoon, *Materials Research Society Symposium - Proceedings* 457 (1997) 81–87.
- [37] S.S. Modhave, K.L. Patil, D.R. Shinde, M.G. Chaskar, R.A. Pawar, *J Emerg Technol Innov Res* 06 (2019) 266–278.
- [38] S. Li, J. Pan, F. Gao, D. Zeng, F. Qin, C. He, G. Dodbiba, Y. Wei, T. Fujita, *Journal of Materials Science: Materials in Electronics* 32 (2021) 13511–13526.
- [39] S. Ikram, J. Jacob, K. Mehboob, K. Mahmood, N. Amin, M.I. Arshad, M. Ajaz un Nabi, *J Supercond Nov Magn* 34 (2021) 1833–1842.
- [40] C. Cao, A. Xia, S. Liu, L. Tong, *Journal of Materials Science: Materials in Electronics* 24 (2013) 4901–4905.
- [41] C. Dan, Z. Huajun, Q. Guangren, Y. Feiqin, G. Changhua, *Huanjing Kexue Xuebao* 27 (2007) 873–879.

- [42] T. Tsoncheva, E. Manova, N. Velinov, D. Paneva, M. Popova, B. Kunev, K. Tenchev, I. Mitov, *Catal Commn* 12 (2010) 105–109.
- [43] C. Sang, S. Jin, G. Li, Y. Luo, *J Solgel Sci Technol* 98 (2021) 559–567.
- [44] S. Liying, W. Yu, J. Zhenbin, *HEBEI CHEMICAL ENGINEERING AND INDUSTRY* (2003) 23–23,26.
- [45] J. Kurian, M. Jacob Mathew, *J Magn Magn Mater* 428 (2017) 204–212.
- [46] C. Cherpin, D. Lister, F. Dacquait, L. Liu, *Materials* 2021, Vol. 14, Page 2557 14 (2021) 2557.
- [47] M. Kurian, *Journal of the Australian Ceramic Society* 59 (2023) 1161–1175.
- [48] M. Latwal, L. Singh, H. Kumar, *Ferrite Nanostructured Magnetic Materials: Technologies and Applications* (2023) 175–196.
- [49] M. Xu, H. Dai, T. Li, K. Peng, J. Chen, Z. Chen, Y. Xue, X. Cao, B. Wang, *J Supercond Nov Magn* 33 (2020) 2881–2890.
- [50] S. Pongpadung, T. Kamwanna, V. Amornkitbamrung, *Journal of the Korean Physical Society* 68 (2016) 697–704.
- [51] N.M. Deraz, *J Anal Appl Pyrolysis* 82 (2008) 212–222.
- [52] S. Deepapriya, P.A. Vinosha, J.D. Rodney, M. Jose, S. Krishnan, J.E. Jose, S.J. Das, *Vacuum* 161 (2019) 5–13.
- [53] G. Dascalu, T. Popescu, M. Feder, O.F. Caltun, *J Magn Magn Mater* 333 (2013) 69–74.
- [54] Q. Lin, G. Yuan, Y. He, L. Wang, J. Dong, Y. Yu, *Mater Des* 78 (2015) 80–84.
- [55] K. Sakthipandi, K. Kannagi, A. Hossain, *Ceram Int* 46 (2020) 19634–19638.
- [56] P.K. Roy, J. Bera, *Mater Res Bull* 42 (2007) 77–83.
- [57] K. Hussain, N. Amin, M.I. Arshad, *Ceram Int* 47 (2021) 3401–3410.
- [58] M. Fatima, M.S.U. Hasan, M. Akhtar, N. Morley, N. Amin, A. ur Rehman, M.I. Arshad, M. Amami, B. Yaqub, S. Ezzine, *ACS Omega* 8 (2023) 41169–41181.
- [59] Yasmin, P.J. Gracie, D. Geetha, *Journal of Materials Science: Materials in Electronics* 35 (2024) 1–20.
- [60] M.S. Khandekar, N.L. Tarwal, J.Y. Patil, F.I. Shaikh, I.S. Mulla, S.S. Suryavanshi, *Ceram Int* 39 (2013) 5901–5907.
- [61] M. Rahimi-Nasrabadi, M. Behpour, A. Sobhani-Nasab, M.R. Jeddy, *Journal of Materials Science: Materials in Electronics* 27 (2016) 11691–11697.
- [62] S. Qamar, M.N. Akhtar, K.M. Batoo, E.H. Raslan, *Ceram Int* 46 (2020) 14481–14487.
- [63] P.V.S. Rao, T. Anjaneyulu, D.V.K. Reddy, M.R. Reddy, P.V.S. Rao, T. Anjaneyulu, D.V.K. Reddy, M.R. Reddy, *Advances in Materials Physics and Chemistry* 8 (2018) 401–410.

- [64] C.B. Kolekar, P.N. Kamble, A.S. Vaingankar, *Indian J. Phys* 68 (1994) 529–537.
- [65] C.B. Kolekar, P.N. Kamble, S.G. Kulkarni, A.S. Vaingankar, *J Mater Sci* 30 (1995) 5784–5788.
- [66] E.E. Ateia, F.S. Soliman, *Appl Phys A Mater Sci Process* 123 (2017) 1–9.
- [67] G. Bulai, V. Trandafir, S.A. Irimiciuc, L. Ursu, C. Focsa, S. Gurlui, *Ceram Int* 45 (2019) 20165–20171.
- [68] B.C. Das, F. Alam, A.K.M.H. Akther, *Journal of Physics and Chemistry of Solids* 142 (2020) 109433.
- [69] R. Rajesh Kanna, K. Sakthipandi, S.M. Seeni Mohamed Aliar Maraikkayar, N. Lenin, M. Sivabharathy, *Journal of Rare Earths* 36 (2018) 1299–1309.
- [70] A. Kiran, M.N. Akhtar, M. Yousaf, K.M. Batoo, O.M. Aldossary, S.N. Khan, *Journal of Rare Earths* 39 (2021) 1224–1231.
- [71] R. Talebi, *Journal of Materials Science: Materials in Electronics* 27 (2016) 6313–6317.
- [72] M.N. Akhtar, M. Babar, S. Qamar, Z. ur Rehman, M.A. Khan, *Ceram Int* 45 (2019) 10187–10195.
- [73] R. Talebi, *Journal of Materials Science: Materials in Electronics* 27 (2016) 6974–6978.
- [74] M.M.N. Ansari, S. Khan, N. Ahmad, *J Alloys Compd* 831 (2020) 154778.
- [75] S. Mahalakshmi, K. SrinivasaManja, S. Nithiyanantham, *Journal of Materials Science: Materials in Electronics* 28 (2017) 3060–3066.
- [76] M. Vosoughifar, A. Kimiay, *Journal of Materials Science: Materials in Electronics* 27 (2016) 10031–10035.
- [77] R.R. Kanna, K. Sakthipandi, N. Lenin, E.J.J. Samuel, *Journal of Materials Science: Materials in Electronics* 30 (2019) 4473–4486.
- [78] M. Mustaqeem, K. Mahmood, T.A. Saleh, A. ur Rehman, M. Ahmad, Z.A. Gilani, M. Asif, *Physica B Condens Matter* 588 (2020) 412176.
- [79] G. Vinod, K. Rajashekhar, J.L. Naik, *Ceram Int* 49 (2023) 2829–2851.
- [80] S. Akbar Hosseini, *Journal of Materials Science: Materials in Electronics* 28 (2017) 1086–1091.
- [81] N. Moeini, A. Alemi, Z. Rezvani, *ChemistrySelect* 7 (2022) e202200275.
- [82] A.A. Khan, S.N. Khan, A. Mir, *J Magn Magn Mater* 559 (2022) 169510.
- [83] K. Manjunatha, B. Chethan, S.Y. Wu, M. Ubaidullah, S.F. Shaikh, A.M. Al-Enizi, N.B. Alanazi, B. Pandit, A. Bajorek, *J. Angadi V, Ceram Int* 49 (2023) 40236–40243.
- [84] E.S. Yousef, I.S. Yahia, H.Y. Zahran, V.J. Angadi, *International Journal of Self-Propagating High-Temperature Synthesis* 31 (2022) 159–163.
- [85] S. Khasim, B.N. Ramakrishna, A. Pasha, S.O. Manjunatha, *J Electron Mater* 53 (2024) 801–814.

- [86] E.E. Ateia, M.K. Abdelmaksoud, M.M. Arman, A.S. Shafaay, Appl Phys A Mater Sci Process 126 (2020) 1–10.
- [87] T. Bian, T. Zhou, Y. Zhang, Energies 2022, Vol. 15, Page 8442 15 (2022) 8442.
- [88] S. Mahalakshmi, K. SrinivasaManja, S. Nithiyanantham, Journal of Superconductivity and Novel Magnetism 2014 27:9 27 (2014) 2083–2088.